



Altered Local Brain Amplitude of Fluctuations in Patients With Myotonic Dystrophy Type 1

Pei Huang^{1†}, Xing-Hua Luan^{1,2†}, Zhou Xie^{3†}, Meng-Ting Li⁴, Sheng-Di Chen¹, Jun Liu¹, Xi-Ze Jia^{4*}, Li Cao^{1,2*} and Hai-Yan Zhou^{1*}

¹ Department of Neurology and Institute of Neurology, Ruijin Hospital, Shanghai Jiao Tong University School of Medicine, Shanghai, China, ² Department of Neurology, Shanghai Jiao Tong University Affiliated Sixth People's Hospital, Shanghai, China, ³ School of Information and Electronics Technology, Jiamusi University, Jiamusi, China, ⁴ Key Laboratory of Intelligent Education Technology and Application of Zhejiang Province, Zhejiang Normal University, Jinhua, China

OPEN ACCESS

Edited by:

Guo-Yuan Yang,
Shanghai Jiao Tong University, China

Reviewed by:

Ma Yuanyuan,
Fudan University, China
Mengzhou Xue,
Zhengzhou University, China

*Correspondence:

Xi-Ze Jia
jiaxize@foxmail.com
Li Cao
caoli2000@yeah.net
Hai-Yan Zhou
zhaiyan.com@163.com

[†]These authors have contributed
equally to this work

Received: 07 October 2021

Accepted: 17 November 2021

Published: 10 December 2021

Citation:

Huang P, Luan X-H, Xie Z, Li M-T,
Chen S-D, Liu J, Jia X-Z, Cao L and
Zhou H-Y (2021) Altered Local Brain
Amplitude of Fluctuations in Patients
With Myotonic Dystrophy Type 1.
Front. Aging Neurosci. 13:790632.
doi: 10.3389/fnagi.2021.790632

This study is aimed at investigating the characteristics of the spontaneous brain activity in patients with myotonic dystrophy type 1 (DM1). A total of 18 patients with DM1 and 18 healthy controls (HCs) were examined by resting-state functional MRI. Combined methods include amplitude of low-frequency fluctuations (ALFFs), the fractional amplitude of low-frequency fluctuations (fALFFs), and Wavelet transform-based ALFFs (Wavelet-ALFFs) with standardization, percent amplitude of fluctuation (PerAF) with/without standardization were applied to evaluate the spontaneous brain activity of patients with DM1. Compared with HCs, patients with DM1 showed decreased ALFFs and Wavelet-ALFFs in the bilateral precuneus (PCUN), angular gyrus (ANG), inferior parietal, but supramarginal and angular gyri (IPL), posterior cingulate gyrus (PCG), superior frontal gyrus, medial (SFGmed), middle occipital gyrus (MOG), which were mainly distributed in the brain regions of default mode network (DMN). Decreased ALFFs and Wavelet-ALFFs were also seen in bilateral middle frontal gyrus (MFG), inferior frontal gyrus, opercular part (IFGoperc), which were the main components of the executive control network (ECN). Patients with DM1 also showed decreased fALFFs in SFGmed.R, the right anterior cingulate and paracingulate gyri (ACGR), bilateral MFG. Reduced PerAF in bilateral PCUN, ANG, PCG, MOG, and IPL as well as decreased PerAF without standardization in PCUNR and bilateral PCG also existed in patients with DM1. In conclusion, patients with DM1 had decreased activity in DMN and ECN with increased fluctuations in the temporal cortex and cerebellum. Decreased brain activity in DMN was the most repeatable and reliable with PCUN and PCG being the most specific imaging biomarker of brain dysfunction in patients with DM1.

Keywords: amplitude of low-frequency fluctuations, resting-state functional MRI, myotonic dystrophy type 1, local brain function, spontaneous brain activity

INTRODUCTION

Myotonic dystrophy type 1 (DM1) is an autosomal dominant hereditary disease caused by the expansion of the cytosine thymine guanine triplet repeats within the myotonic dystrophy protein of the kinase (DMPK) gene. The prevalence of DM1 ranges from 0.5 to 18.1 per 100,000 population, making it the most common muscular dystrophy disease (Theadom et al., 2014). DM1 can present

at any age but is typically diagnosed in adults with many different ways of presentation, such as facial and distal muscle weakness, along with grip myotonia. It was primarily recognized as a disease-affecting muscular function, whereas many patients also experienced multiple symptoms including cognitive impairment, apathy, sleep disorders, and behavioral disturbances (Theadom et al., 2014; Okkersen et al., 2017a).

Neurological involvement in the DM1 has aroused lots of interest in the recent years and several brain MRI studies have reported white matter lesions and brain atrophy (Minnerop et al., 2011; Baldanzi et al., 2016; Zanigni et al., 2016; Okkersen et al., 2017b; Kosciak et al., 2021; Leddy et al., 2021; Lopez-Titla et al., 2021). Diffusion tensor imaging studies have demonstrated widespread white matter lesions with reduced fractional anisotropy (FA) and increased mean diffusivity in patients with DM1 compared with controls (Cabada et al., 2017; Yoo et al., 2017; van Dorst et al., 2019). Widespread reduction of gray matter volume (including frontal, temporal, parietal, and occipital cortices, as well as deep gray matter structures and cerebellum) was found in patients with DM1 using the voxel-based morphometry method (Minnerop et al., 2011; Baldanzi et al., 2016; Zanigni et al., 2016; Hamilton et al., 2018; Park et al., 2018; Gliem et al., 2019; Labayru et al., 2019, 2020; Serra et al., 2020a; Cabada et al., 2021). Recent studies have investigated abnormalities in gray matter structural networks using graph theoretical analysis. Frontal disconnection and increased parietal-cerebellar connectivity were identified in the brains of the patients (Serra et al., 2016a,b; Cabada et al., 2017; Sugiyama et al., 2017; Yoo et al., 2017). However, even with such widespread white matter lesions and brain atrophy, some general cognitive function of patients with DM1 were still preserved (Gaul et al., 2006). It indicates that structural measurements are not able to accurately reflect the changes of the brain function, investigation of brain functional changes in patients with DM1 is urgent.

Till now, very few studies have focused on the functional analysis of brain MRI in DM1 patients (Serra et al., 2014, 2020b). Previous studies using motor-task-related fMRI had found altered activation patterns in bilateral motor regions in patients with DM1 (Caramia et al., 2010; Toth et al., 2015). The resting-state fMRI study focusing on brain functional connectivity had reported abnormal functional connectivity in default mode network (DMN) in relation to deficits of personality traits and social cognition (Serra et al., 2014). Although brain functional connectivity analysis gave us an in-depth understanding of brain impairments in patients with DM1, it could not reflect local brain function change, which made it difficult to localize the responsible brain damage.

To specifically localize the brain regions with abnormal activity, the amplitude of low-frequency fluctuations (ALFFs) is a reliable approach to monitor spontaneous neuronal fluctuations and can reflect cerebral physiological states and local brain functions (Zang et al., 2007). However, each method has its own advantages and limitations. As we know, ALFFs have been widely applied to the resting-state fMRI studies of the neurological diseases, but it could be easily influenced by noise signals (Zuo et al., 2010). To effectively inhibit non-specific signal

components of resting-state fMRI, fractional amplitude low-frequency fluctuations (fALFFs) are applied to measure a range of low frequency (0.01–0.08 Hz) divided by the entire frequency range (Zou et al., 2008). Compared with ALFFs calculated with fast Fourier transform (FFT), wavelet transform (WT)-based ALFFs (Wavelet-ALFFs) is more effective in depicting the complex time series (Luo et al., 2020). In addition, the percent amplitude of fluctuation (PerAF) was proved to have good reliability in investigating the abnormal BOLD signal in resting-state fMRI (Jia et al., 2020).

Thus, this study aims to investigate the local spontaneous brain activity of patients with DM1 using combined methods of the amplitude of low-frequency fluctuations, such as ALFFs, fALFFs, Wavelet-ALFFs, PerAF with/without global mean standardization. We want to discover the most reliable abnormal changes of the local brain function in patients with DM1.

MATERIALS AND METHODS

Participants

Diagnosis of DM1 was based on clinical features and electromyographic evidence of myopathy and myotonia. A total of 18 patients with DM1 were enrolled and all the cases were genetically confirmed. The inclusion criteria for patients were as follows: (1) right-handed according to Edinburgh Handedness Inventory (Oldfield, 1971); (2) age ranging from 20 to 80 years; and (3) genetically confirmed cases of DM1. Exclusion criteria included: (1) history of drug and alcohol abuse; (2) brain damage, such as head trauma and history of stroke; (3) other diseases that cause muscle weakness, such as myositis, myasthenia gravis, and peripheral neuropathy; and (4) MRI incompatibility. A total of 18 healthy controls (HCs) demographically matched with patients in terms of age, sex, and years of education were recruited.

All the participants were fully informed and signed written consent forms. This study was approved by the Ethic Committee of the Ruijin Hospital Affiliated to the Shanghai Jiao Tong University School of Medicine, and registered on the Chinese clinical trial registry (ChiCTR2000032978).

Clinical Examinations

All the participants were evaluated by neurologists. Cognition and depression were assessed by the Mini-Mental State Examination (MMSE) and the Hamilton Depression Scale-17 (HAMD-17). The patients also accepted electromyographic testing and genetic testing.

Magnetic Resonance Imaging Data Acquisition

A total of 18 patients with DM1 and 18 HC participated in rs-fMRI scan on a 3.0 Tesla GE Medical System (GE Healthcare, Little Chalfont, United Kingdom) scanner. During the scan, the subjects were asked to remain motionless and awake with their eyes closed. For each participant, 210 functional

images were collected using blood oxygen level dependent (BOLD) sequence [repetition time (TR) = 2,000 ms; echo time (TE) = 30 ms; flip angle = 90°; 35 slices; matrix = 64 × 64; voxel size = 3.75 mm³ × 3.75 mm³ × 4 mm³]. Then, the high-resolution, three-dimensional, T1-weighted structural images (TR = 5.5 ms; TE = 1.7 ms; flip angle = 12°; matrix = 256 × 256; voxel size = 1 mm³ × 1 mm³ × 1 mm³) were acquired for the registration and normalization of the functional images.

Magnetic Resonance Imaging Data Pre-processing

Image data pre-processing was carried out using RESTplus V1.24¹ (Jia et al., 2019) and SPM12.² The pre-processing steps included: (1) removing the first 10 time points; (2) slice timing correction; and (3) realigning. Participants of head motion exceeding 3 mm or 3° were excluded. Finally, two patients with DM1 were excluded; (4) First, an individual structural image was coregistered to the mean functional image, and then it was segmented into tissue segmentation of the structural images. The Diffeomorphic Anatomical Registration Through Exponentiated Lie Algebra (DARTEL) tool was used to compute the transformation from individual space to MNI space and vice-versa (resampling voxel size = 3 mm × 3 mm × 3 mm); (5) Smooth. Spatial smoothing with a Gaussian kernel of 6 mm full-width at half-maximum (FWHM) to explore the influence of different smooth kernel on the results, we also smoothed the fMRI data with a 4 mm FWHM; (6) Removing the linear trend of the time series; (7) Regressing out nuisance variables, including Friston-24 head motion parameters (Friston et al., 1996; Jenkinson et al., 2002), the cerebrospinal flow signals, and white matter signals. The mean value of the time series of each voxel was added back in this step; considering the influence of the global brain signals (Macey et al., 2004; Fox et al., 2009), we also regressed out the global mean signals to see the data stability; (8) Band-pass filtering (0.01–0.08 Hz), this step of pre-processing was only done in PerAF.

Magnetic Resonance Imaging Data Processing

Magnetic resonance imaging data of 16 patients with DM1 and 18 HC were enrolled into the next analysis. The ALFFs and fALFFs analyses were performed using the RESTplus V1.24. After pre-processing, the time series of each voxel was transformed to the frequency domain by the fast Fourier transform (FFT), and the power spectrum was obtained. The square root was calculated at each frequency of the power spectrum. The average square root across 0.01–0.08 Hz was taken as ALFFs of each voxel (Zang et al., 2007). The ratio of the sum of amplitude within the 0.01–0.08 Hz to that of the whole frequency band was calculated as fALFFs (Zou et al., 2008). For standardization, the ALFFs and fALFFs value of each voxel was divided by the global mean ALFFs and the global mean fALFFs within the brain mask separately.

The PerAF of each voxel was calculated as follows (Jia et al., 2020),

$$\text{PerAF} = \frac{1}{n} \sum_{i=1}^n \left| \frac{X_i - \mu}{\mu} \right| \times 100\%$$

$$\mu = \frac{1}{n} \sum_{i=1}^n X_i$$

where X_i is the signal intensity of the i_{th} time point, n is the total number of time points of the time series, and μ is the mean value of the time series. The PerAF of each voxel was then divided by the global mean of the PerAF values for standardization.

Wavelet-ALFFs calculation was based on continuous WT (CWT). Wavelet-ALFFs was calculated by first adding up the wavelet coefficients at all time points for each frequency point, and the averaged coefficient across a given frequency band was then obtained as defined later (Luo et al., 2020):

$$\text{Wavelet-ALFF} = \frac{1}{m} \sum_{i=1}^n |CWT_{i,j}|, \quad j = s_1 \dots s_m$$

where $|CWT_{i,j}|$ denotes the absolute value of wavelet coefficient at time point i at a given frequency point j ; n denotes the total amount of wavelet coefficient at a given frequency point; and m denotes the total number of frequency points across a given frequency band. The Wavelet-ALFFs of each voxel was then divided by the global mean of the Wavelet-ALFFs values for standardization. In this study, we calculated the Wavelet-ALFFs in the conventional frequency band of 0.01–0.08 Hz.

Statistical Analysis

The two-sample t -test was performed in the demographic data of both the groups in SPSS (version 24.0, Armonk, New York, United States). All the tests of demographics were two-tailed and $p < 0.05$ was considered significant. The ALFFs, fALFFs, and Wavelet-ALFFs with standardization, PerAF with/without standardization were analyzed by an independent two-sample t -test in the DPABI V5.1³ (Yan et al., 2016). The permutation test with a threshold-free cluster enhancement (TFCE) (Chen et al., 2018) (number of permutations = 5,000) method was used in the two-sample t -test, and the comparison was done between patients and control group in gray matter mask. A $P < 0.01$ and cluster size threshold ≥ 10 voxels was considered statistically significant (FWE corrected). In addition, since the head motion is an important confounding factor in fMRI studies (Satterthwaite et al., 2012; Zeng et al., 2014), the frame-wise displacement (FD) parameter was regressed out in the two-sample t -test of all the five metrics, and results were thresholded with the TFCE ($P_{FWE} < 0.01$, number of permutations was set as 5,000 with a minimum cluster size = 10).

¹<http://restfmri.net/forum/restplus>

²<https://www.fil.ion.ucl.ac.uk/spm/>

³<http://rfmri.org/dpabi>

RESULTS

Demographics and Clinical Characteristics

A total of 18 patients with DM1 and 18 HCs were enrolled in the study, while 2 patients with DM1 were excluded because of head motion. 16 patients with DM1 and 18 HCs were included into the final analysis. They were matched in age ($p = 0.114$), gender ($p = 0.510$), and education ($p = 0.121$), but patients with DM1 showed significantly lower score in MMSE ($p < 0.001$) and higher score in HAMD-17 ($p < 0.001$) than HCs (Table 1).

Group Differences in Amplitude of Low-Frequency Fluctuations

Compared with HC, patients with DM1 showed increased ALFFs in the left inferior temporal gyrus (ITGL), left parahippocampal gyrus (PHGL), right fusiform gyrus (FFGR), right inferior cerebellum (Cerebelum_8R); and decreased ALFFs in the right precuneus (PCUNR), bilateral angular gyrus (ANG), left inferior parietal, but supramarginal and angular gyri (IPLL), left posterior cingulate gyrus (PCGL), bilateral superior frontal gyrus, medial (SFGmed), right middle occipital gyrus (MOGR). Decreased ALFFs were also seen in bilateral middle frontal gyrus (MFG), left inferior frontal gyrus, opercular part (IFGopercL) and also the right median cingulate and paracingulate gyri (DCGR) (Table 2 and Figure 1A).

Group Differences in Fractional Amplitude of Low-Frequency Fluctuations

Compared with HC, patients with DM1 showed decreased fALFFs in SFGmedR. The right anterior cingulate and paracingulate gyri (ACG.R), bilateral MFG also presented decreased fALFFs as well as the right supplementary motor area (SMA.R) (Table 2 and Figure 1B).

Group Differences in Wavelet-Amplitude of Low-Frequency Fluctuations

Compared with HC, patients with DM1 showed increased Wavelet-ALFFs in ITGL, PHGL, Cerebelum_8L, and Vermis_9 and decreased Wavelet-ALFFs in bilateral PCUN, bilateral ANG, bilateral IPL, PCGR, bilateral SFGmed, and bilateral MOG.

Bilateral MFG, bilateral IFGoperc, ACGR, and the right middle temporal gyrus (MTGR) also presented decreased Wavelet-ALFFs (Table 2 and Figure 1C).

Group Differences in Percent Amplitude of Fluctuation

Compared with HC, patients with DM1 showed decreased PerAF in bilateral PCUN, bilateral ANG, IPLL, bilateral PCG, and bilateral MOG (Table 2 and Figure 1D).

Group Differences in Percent Amplitude of Fluctuation Without Standardization

Compared with HC, patients with DM1 showed decreased PerAF without standardization in PCUN.R and bilateral PCG. In addition, DCG.R also presented decreased PerAF without standardization (Table 2 and Figure 1E).

Data Stability

The result patterns of all the 5 metrics before and after the regression of FD parameters were similar, which indicated weak influence of head motion on the results (see Supplementary Figures 1, 4, 7, 10, 13). After regressing out the global mean signals, the result patterns of all the five metrics also remained similar (see Supplementary Figures 2, 5, 8, 11, 14). The result patterns of all the five metrics with two FWHM Gaussian kernel were consistent, which also indicated the stability of our results (see Supplementary Figures 3, 6, 9, 12, 15).

DISCUSSION

This study found that patients with DM1 had decreased amplitude of brain spontaneous activity in PCUN, ANG, IPL, PCG, SFGmed, and MOG, which were the major components of DMN. Spontaneous brain fluctuations in MFG, IFGoperc, ACG, and MTG, which were the main components of the executive control network (ECN), also showed a decreased pattern. Other brain regions, such as SMA and DCG also presented decreased brain activity in patients with DM1 compared with HC. Abnormal increased brain fluctuations were found in ITG, PHG, FFG, cerebelum_8, and vermis_9. Among all the abnormal changes in amplitude of low-frequency fluctuations based on four different methods, such as ALFFs, fALFFs, Wavelet-ALFFs and PerAF with/without standardization, decreased brain activity in DMN was the most reliable and robust result.

Default mode network includes bilateral ventromedial prefrontal cortex, dorsomedial prefrontal cortex, posterior cingulate cortex and adjacent precuneus, as well as the lateral parietal cortex (Biswal et al., 1995; Brown et al., 2019). The DMN is a set of regions that are most active at rest and decrease in activity during externally directed tasks (Brown et al., 2019). The DMN is thought to be primarily responsible for internally focused thought processes, such as autobiographical memory and experience of the self, which is an important contributor to executive function performance (Chand et al., 2017). Age-related reduction in DMN deactivation is associated with poorer

TABLE 1 | Demographics and clinical characteristics of the subjects.

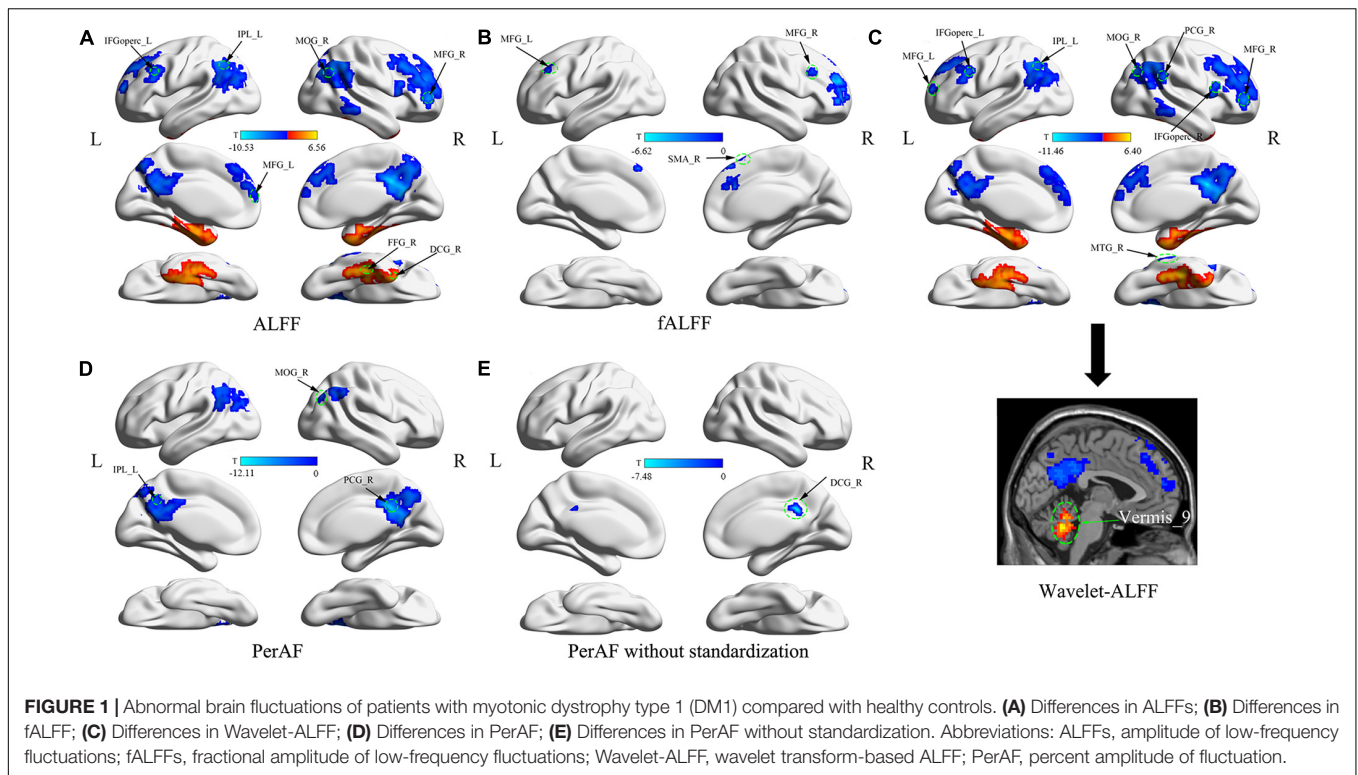
Characteristics	DM1 (n = 16)	HC (n = 18)	p value
Age (y)	48.44 ± 14.14	41.50 ± 10.67	0.114
Gender (M/F)	10/6	9/9	0.510
Education (y)	13.00 ± 3.16	14.56 ± 2.53	0.121
Disease duration (y)	6.19 ± 4.82	—	—
MMSE	27.06 ± 1.84	29.17 ± 0.92	<0.001
HAMD-17	6.00 ± 4.23	2.06 ± 0.80	<0.001

Abbreviations: DM1, myotonic dystrophy type 1; HC, healthy control; MMSE, Mini-Mental State Examination; HAMD-17, Hamilton Depression Scale-17.

TABLE 2 | Brain regions showing differences in ALFFs, fALFFs, Wavelet-ALFFs, and PerAF with/without standardization between the groups.

Metric	Cluster	Brain regions	L/R	Cluster size	BA	Peak MNI coordinates			Peak intensity (t)	
						X	Y	Z		
ALFF	1	FFG	R	2200	/	42	-24	-24	6.5566	
		Cerebellum_8	R	232						
		ITG	L	160						
		PHG	L	71						
	2	MOG	R	689	/	36	-72	36	-7.4354	
		ANG	R	229						
	3	PCUN	R	82						
		DCG	R	903	31	3	-42	39	-10.5306	
		PCUN	R	305						
	4	PCG	L	75						
		MFG	R	1309	/	42	48	3	-6.7737	
	5	SFGmed	L	149						
		SFGmed	R	141						
	6	IPL	L	580	/	-45	-54	45	-6.7280	
ANG		L	176							
7	MFG	L	22	10	-27	60	15	-5.7711		
	IFGoperc	L	73	/	-42	18	33	-4.7665		
fALFF	1	MFG	L	34						
		SMA	R	380	/	6	24	63	-6.6199	
		MFG	R	155						
		SFGmed	R	63						
	2	ACG	R	5						
		MFG	R	10	9	39	21	33	-5.2016	
	3	MFG	L	20	9	-45	27	39	-4.6801	
	Wavelet-ALFF	1	Vermis_9	/	2102	/	-3	-57	-33	6.3959
			Cerebellum_8	L	233					
			ITG	L	148					
			PHG	L	67					
		2	MTG	R	65	/	66	-42	0	-5.4868
			PCG	R	752	/	6	-42	30	-11.4574
		3	PCUN	R	241					
PCUN			L	183						
MFG			R	1113	/	42	48	3	-6.7995	
4		SFGmed	L	170						
		SFGmed	R	134						
5		ACG	R	7						
		MFG	L	11	10	-27	60	15	-5.6510	
6		IPL	L	522	/	-45	-54	45	-7.0722	
	ANG	L	164							
7	MOG	L	143							
	IFGoperc	R	77	/	48	15	15	-5.2355		
8	MOG	R	494	/	36	-72	36	-7.5466		
	ANG	R	195							
9	IPL	R	113							
	IFGoperc	L	63	/	-42	18	33	-4.7363		
PerAF	1	PCG	R	773	31	3	-42	30	-12.113	
		PCUN	R	244						
		PCUN	L	186						
		PCG	L	72						
	2	IPL	L	484	40	-45	-51	42	-6.6327	
		MOG	L	170						
		ANG	L	149						
	3	MOG	R	208	/	36	-72	36	-6.5362	
		ANG	R	90						
	PerAF without standardization	1	DCG	R	38	31	3	-39	33	-7.4807
			PCG	R	6					
			PCG	L	3					
			PCUN	R	1					

Abbreviations: MNI, Montreal Neurological Institute; BA, Brodmann area; ALFF, amplitude of low-frequency fluctuations; fALFF, fractional amplitude of low-frequency fluctuations; Wavelet-ALFF, wavelet transform-based ALFF; PerAF, percent amplitude of fluctuation; FFG, fusiform gyrus; ITG, inferior temporal gyrus; PHG, parahippocampal gyrus; MOG, middle occipital gyrus; ANG, angular gyrus; PCUN, precuneus; DCG, median cingulate and paracingulate gyri; PCG, posterior cingulate gyrus; MFG, middle frontal gyrus; SFGmed, superior frontal gyrus medial; IPL, inferior parietal; IFGoperc, inferior frontal gyrus, opercular part; SMA, supplementary motor area; ACG, anterior cingulate and paracingulate gyri; MTG, middle temporal gyrus.



executive function task performance (Brown et al., 2015). Patients with DM1 were reported to have significant decrease in executive function (Gaul et al., 2006; Filli et al., 2020). Our study found decreased brain activity in PCUN, ANG, IPL, PCG, SFGmed, and MOG, which mainly distributed in brain regions of the DMN. Based on the results from four different methods of analyzing amplitude of low-frequency fluctuations, decreased brain activity in DMN was the most reliable and robust. Previous studies of brain functional connectivity using rs-fMRI reported abnormal functional connectivity in DMN, which was related to patients with DM1 deficits of personality traits and social cognition (Buckner et al., 2005; Lenzoni et al., 2020). This study further localized the abnormally functioned brain regions by analyzing the local brain fluctuations, which helped us further understanding the pathogenesis of the disease.

Brain regions correlated with ECN, such as MFG, IFGoperc, ACG, and MTG, also presented decreased brain fluctuations. Regions within the ECN include anterior cingulate cortex/pre-supplementary motor area (ACC/pre-SMA), dorsolateral prefrontal cortex, inferior frontal junction, anterior insular cortex, dorsal premotor cortex, and posterior parietal cortex (Cole and Schneider, 2007; Xu et al., 2020). ECN is widely reported to be more activated for externally directed higher-order cognitive functions, such as attention, working memory, and decision-making (Bressler and Menon, 2010). The functional cross-talk between DMN and ECN networks mirrors the integrity of cognitive processing and is directly related to brain development (Fu et al., 2021; Xue et al., 2021). Low DMN deactivation and high ECN activation were suggested to be the main predictors of executive dysfunction (Della Rosa et al., 2021).

This study indicated that ECN, especially such brain regions as MFG, IFGoperc, ACG, and MTG might play an important role in patients with DM1 brain dysfunction.

Other brain regions such as SMA and DCG also presented decreased the brain activity in patients with DM1 compared with HC. Considered as a main component of cognitive control network, SMA might connect with ECN through pre-SMA (Niendam et al., 2012), participate in automatic motor actions (Nee et al., 2007), and modulate interhemispheric interactions (Welniaz et al., 2019). Abnormal functional connectivity between DCG and dorsal anterior insular was related to deficits in attention/working memory and visuospatial function (Pan et al., 2021). Further investigation is needed to explore the relationship between abnormal brain activity in SMA and DCG and the cognitive deficits of patients with DM1.

Abnormal pattern of the brain activity in patients with DM1 also includes increased brain fluctuations in ITG, PHG, FFG, cerebelum_8, and vermis_9, which are mainly distributed in the temporal cortex and cerebellum. Previous studies demonstrate that ITG, PHG, and FFG were associated with emotion processing (Liao et al., 2011; Müller et al., 2012). The lobule VIII of the cerebellum was connected with the sensorimotor network and the vermis was involved in emotion function (Schmahmann, 2019). Although their underlying pathophysiological mechanism is unclear, abnormal local brain fluctuations in ITG, PHG, FFG, cerebelum_8, and vermis may correlate with emotional deficits of patients with DM1.

Aforementioned results were confirmed with the combination of different methods of evaluating local brain fluctuation. As we know, each method has its advantages and limitations. In

our study, decreased brain activity in DMN and ECN, especially in PCUN and PCG, was consistent among different methods. What is more that the results were stable after considering the influence of head motion, global brain signals, and different smooth kernel. Thus, decreased local brain fluctuation in PCUN and PCG was considered the most reliable and robust change in patients with DM1.

LIMITATIONS

The limitation of this study is the relatively small sample size, and larger cohort is needed to confirm the results in the future studies. However, the prevalence of DM1 ranges from 0.5 to 18.1 per 100,000 population and belongs to rare disease, and the local brain function of patients with DM1 has not been investigated previously. What is important is that reliable and stable changes in PCUN and PCG of patients with DM1 are confirmed based on the consistent results among different methods. This study provides good evidence of altered amplitude of fluctuations in DMN and ECN, especially in PCUN and PCG areas. We attend to further explore the cognitive and emotional changes in patients with DM1, and decipher the relationship between clinical presentations and brain functional changes in a larger scale sample.

CONCLUSION

Patients with DM1 had decreased activity in DMN and ECN with increased fluctuations in the temporal cortex and cerebellum. Decreased brain activity in DMN was the most reliable with PCUN and PCG being the most robust brain regions.

DATA AVAILABILITY STATEMENT

The raw data supporting the conclusions of this article will be made available by the authors, without undue reservation.

REFERENCES

- Baldanzi, S., Cecchi, P., Fabbri, S., Pesaresi, I., Simoncini, C., Angelini, C., et al. (2016). Relationship between neuropsychological impairment and grey and white matter changes in adult-onset myotonic dystrophy type 1. *Neuroimage Clin.* 12, 190–197. doi: 10.1016/j.nicl.2016.06.011
- Biswal, B., Yetkin, F. Z., Haughton, V. M., and Hyde, J. S. (1995). Functional connectivity in the motor cortex of resting human brain using echo-planar MRI. *Magn. Reson. Med.* 34, 537–541. doi: 10.1002/mrm.1910340409
- Bressler, S. L., and Menon, V. (2010). Large-scale brain networks in cognition: emerging methods and principles. *Trends Cogn. Sci.* 14, 277–290. doi: 10.1016/j.tics.2010.04.004
- Brown, C. A., Hakun, J. G., Zhu, Z., Johnson, N. F., and Gold, B. T. (2015). White matter microstructure contributes to age-related declines in task-induced deactivation of the default mode network. *Front. Aging Neurosci.* 7:194. doi: 10.3389/fnagi.2015.00194
- Brown, C. A., Schmitt, F. A., Smith, C. D., and Gold, B. T. (2019). Distinct patterns of default mode and executive control network circuitry contribute to present and future executive function in older adults. *Neuroimage* 195, 320–332. doi: 10.1016/j.neuroimage.2019.03.073

ETHICS STATEMENT

The studies involving human participants were reviewed and approved by the Ethics Committee of Ruijin Hospital Affiliated to Shanghai Jiao Tong University School of Medicine. The patients/participants provided their written informed consent to participate in this study.

AUTHOR CONTRIBUTIONS

H-YZ, LC, PH, X-HL, and X-ZJ gave study conceptualization and design. PH and X-HL were involved in data collection. PH, ZX, X-HL, X-ZJ, and M-TL helped with data analysis and interpretation. LC, H-YZ, S-DC, and JL contributed to the supervision of the study procedures. PH and ZX contributed to drafting the manuscript. All authors contributed to the final version of the manuscript.

FUNDING

This study was supported by grants from the National Natural Science Foundation of China (81801267, 81870889, 82071258, and 82001898).

ACKNOWLEDGMENTS

Thanks to all the subjects for participation.

SUPPLEMENTARY MATERIAL

The Supplementary Material for this article can be found online at: <https://www.frontiersin.org/articles/10.3389/fnagi.2021.790632/full#supplementary-material>

- Buckner, R. L., Snyder, A. Z., Shannon, B. J., LaRossa, G., Sachs, R., Fotenos, A. F., et al. (2005). Molecular, structural, and functional characterization of Alzheimer's disease: evidence for a relationship between default activity, amyloid, and memory. *J. Neurosci.* 25, 7709–7717. doi: 10.1523/jneurosci.2177-05.2005
- Cabada, T., Díaz, J., Iridoy, M., López, P., Jericó, I., Lecumberri, P., et al. (2021). Longitudinal study in patients with myotonic dystrophy type 1: correlation of brain MRI abnormalities with cognitive performances. *Neuroradiology* 63, 1019–1029. doi: 10.1007/s00234-020-02611-9
- Cabada, T., Iridoy, M., Jericó, I., Lecumberri, P., Seijas, R., Gargallo, A., et al. (2017). Brain involvement in myotonic dystrophy type 1: a morphometric and diffusion tensor imaging study with neuropsychological correlation. *Arch. Clin. Neuropsychol.* 32, 401–412. doi: 10.1093/arclin/acx008
- Caramia, F., Mainero, C., Gagnani, F., Tinelli, E., Fiorelli, M., Ceschin, V., et al. (2010). Functional MRI changes in the central motor system in myotonic dystrophy type 1. *Magn. Reson. Imaging* 28, 226–234. doi: 10.1016/j.mri.2009.07.006
- Chand, G. B., Wu, J., Hajjar, I., and Qiu, D. (2017). Interactions of the salience network and its subsystems with the default-mode and the central-executive

- networks in normal aging and mild cognitive impairment. *Brain Connect.* 7, 401–412. doi: 10.1089/brain.2017.0509
- Chen, X., Lu, B., and Yan, C. G. (2018). Reproducibility of R-fMRI metrics on the impact of different strategies for multiple comparison correction and sample sizes. *Hum. Brain Mapp.* 39, 300–318. doi: 10.1002/hbm.23843
- Cole, M. W., and Schneider, W. (2007). The cognitive control network: integrated cortical regions with dissociable functions. *Neuroimage* 37, 343–360. doi: 10.1016/j.neuroimage.2007.03.071
- Della Rosa, P. A., Canini, M., Marchetta, E., Cirillo, S., Pontesilli, S., Scotti, R., et al. (2021). The effects of the functional interplay between the default mode and executive control resting state networks on cognitive outcome in preterm born infants at 6 months of age. *Brain Cogn.* 147:105669. doi: 10.1016/j.bandc.2020.105669
- Filli, L., Schwegler, S., Meyer, C., Killeen, T., Easthope, C. S., Broicher, S. D., et al. (2020). Characterizing cognitive-motor impairments in patients with myotonic dystrophy type 1. *Neuromuscul. Disord.* 30, 510–520. doi: 10.1016/j.nmd.2020.04.005
- Fox, M. D., Zhang, D., Snyder, A. Z., and Raichle, M. E. (2009). The global signal and observed anticorrelated resting state brain networks. *J. Neurophysiol.* 101, 3270–3283. doi: 10.1152/jn.90777.2008
- Friston, K. J., Williams, S., Howard, R., Frackowiak, R. S., and Turner, R. (1996). Movement-related effects in fMRI time-series. *Magn. Reson. Med.* 35, 346–355. doi: 10.1002/mrm.1910350312
- Fu, Z., Zhao, M., He, Y., Wang, X., Lu, J., Li, S., et al. (2021). Divergent connectivity changes in gray matter structural covariance networks in subjective cognitive decline, amnesic mild cognitive impairment, and alzheimer's disease. *Front. Aging Neurosci.* 13:686598. doi: 10.3389/fnagi.2021.686598
- Gaul, C., Schmidt, T., Windisch, G., Wieser, T., Müller, T., Vielhaber, S., et al. (2006). Subtle cognitive dysfunction in adult onset myotonic dystrophy type 1 (DM1) and type 2 (DM2). *Neurology* 67, 350–352. doi: 10.1212/01.wnl.0000225180.27833.c1
- Gliem, C., Minnerop, M., Roeske, S., Gärtner, H., Schoene-Bake, J. C., Adler, S., et al. (2019). Tracking the brain in myotonic dystrophies: a 5-year longitudinal follow-up study. *PLoS One* 14:e0213381. doi: 10.1371/journal.pone.0213381
- Hamilton, M. J., McLean, J., Cumming, S., Ballantyne, B., McGhie, J., Jampana, R., et al. (2018). Outcome measures for central nervous system evaluation in myotonic dystrophy type 1 may be confounded by deficits in motor function or insight. *Front. Neurol.* 9:780. doi: 10.3389/fneur.2018.00780
- Jenkinson, M., Bannister, P., Brady, M., and Smith, S. (2002). Improved optimization for the robust and accurate linear registration and motion correction of brain images. *Neuroimage* 17, 825–841. doi: 10.1016/s1053-8119(02)91132-8
- Jia, X. Z., Sun, J. W., Ji, G. J., Liao, W., Lv, Y. T., Wang, J., et al. (2020). Percent amplitude of fluctuation: a simple measure for resting-state fMRI signal at single voxel level. *PLoS One* 15:e0227021. doi: 10.1371/journal.pone.0227021
- Jia, X. Z., Wang, J., Sun, H. Y., Zhang, H., and Zang, Y. F. (2019). RESTplus: an improved toolkit for resting-state functional magnetic resonance imaging data processing. *Sci. Bull.* 64, 953–954. doi: 10.1016/j.scib.2019.05.008
- Koscik, T. R., van der Plas, E., Gutmann, L., Cumming, S. A., Monckton, D. G., Magnotta, V., et al. (2021). White matter microstructure relates to motor outcomes in myotonic dystrophy type 1 independently of disease duration and genetic burden. *Sci. Rep.* 11:4886. doi: 10.1038/s41598-021-84520-2
- Labayru, G., Diez, I., Sepulcre, J., Fernández, E., Zulaica, M., Cortés, J. M., et al. (2019). Regional brain atrophy in gray and white matter is associated with cognitive impairment in myotonic dystrophy type 1. *Neuroimage Clin.* 24:102078. doi: 10.1016/j.nicl.2019.102078
- Labayru, G., Jimenez-Marin, A., Fernández, E., Villanua, J., Zulaica, M., Cortes, J. M., et al. (2020). Neurodegeneration trajectory in pediatric and adult/late DM1: a follow-up MRI study across a decade. *Ann. Clin. Transl. Neurol.* 7, 1802–1815. doi: 10.1002/acn3.51163
- Leddy, S., Serra, L., Esposito, D., Vizzotto, C., Giulietti, G., Silvestri, G., et al. (2021). Lesion distribution and substrate of white matter damage in myotonic dystrophy type 1: comparison with multiple sclerosis. *Neuroimage Clin.* 29:102562. doi: 10.1016/j.nicl.2021.102562
- Lenzoni, S., Bozzoni, V., Burgio, F., de Gelder, B., Wennberg, A., Botta, A., et al. (2020). Recognition of emotions conveyed by facial expression and body postures in myotonic dystrophy (DM). *Cortex* 127, 58–66. doi: 10.1016/j.cortex.2020.02.005
- Liao, W., Xu, Q., Mantini, D., Ding, J., Machado-de-Sousa, J. P., Hallak, J. E., et al. (2011). Altered gray matter morphometry and resting-state functional and structural connectivity in social anxiety disorder. *Brain Res.* 1388, 167–177. doi: 10.1016/j.brainres.2011.03.018
- Lopez-Titla, M. M., Chirino, A., Cruz Solis, S. V., Hernandez-Castillo, C. R., Diaz, R., Márquez-Quiroz, L. D. C., et al. (2021). Cognitive decline and white matter integrity degradation in myotonic dystrophy type I. *J. Neuroimaging* 31, 192–198. doi: 10.1111/jon.12786
- Luo, F. F., Wang, J. B., Yuan, L. X., Zhou, Z. W., Xu, H., Ma, S. H., et al. (2020). Higher sensitivity and reproducibility of wavelet-based amplitude of resting-state fMRI. *Front. Neurosci.* 14:224. doi: 10.3389/fnins.2020.00224
- Macey, P. M., Macey, K. E., Kumar, R., and Harper, R. M. (2004). A method for removal of global effects from fMRI time series. *Neuroimage* 22, 360–366. doi: 10.1016/j.neuroimage.2003.12.042
- Minnerop, M., Weber, B., Schoene-Bake, J. C., Roeske, S., Mirbach, S., Anspach, C., et al. (2011). The brain in myotonic dystrophy 1 and 2: evidence for a predominant white matter disease. *Brain* 134(Pt 12), 3530–3546. doi: 10.1093/brain/awr299
- Müller, V. I., Cieslik, E. C., Turetsky, B. I., and Eickhoff, S. B. (2012). Crossmodal interactions in audiovisual emotion processing. *Neuroimage* 60, 553–561. doi: 10.1016/j.neuroimage.2011.12.007
- Nee, D. E., Wager, T. D., and Jonides, J. (2007). Interference resolution: insights from a meta-analysis of neuroimaging tasks. *Cogn. Affect. Behav. Neurosci.* 7, 1–17. doi: 10.3758/cabn.7.1.1
- Niendam, T. A., Laird, A. R., Ray, K. L., Dean, Y. M., Glahn, D. C., and Carter, C. S. (2012). Meta-analytic evidence for a superordinate cognitive control network subserving diverse executive functions. *Cogn. Affect. Behav. Neurosci.* 12, 241–268. doi: 10.3758/s13415-011-0083-5
- Okkersen, K., Buskes, M., Groenewoud, J., Kessels, R. P. C., Knoop, H., van Engelen, B., et al. (2017a). The cognitive profile of myotonic dystrophy type 1: a systematic review and meta-analysis. *Cortex* 95, 143–155. doi: 10.1016/j.cortex.2017.08.008
- Okkersen, K., Monckton, D. G., Le, N., Tuladhar, A. M., Raaphorst, J., and van Engelen, B. G. M. (2017b). Brain imaging in myotonic dystrophy type 1: a systematic review. *Neurology* 89, 960–969. doi: 10.1212/wnl.0000000000004300
- Oldfield, R. C. (1971). The assessment and analysis of handedness: the edinburgh inventory. *Neuropsychologia* 9, 97–113. doi: 10.1016/0028-3932(71)90067-4
- Pan, C., Ren, J., Li, L., Li, Y., Xu, J., Xue, C., et al. (2021). Differential functional connectivity of insular subdivisions in de novo Parkinson's disease with mild cognitive impairment. *Brain Imaging Behav.* doi: 10.1007/s11682-021-00471-2
- Park, J. S., Song, H., Jang, K. E., Cha, H., Lee, S. H., Hwang, S. K., et al. (2018). Diffusion tensor imaging and voxel-based morphometry reveal corticospinal tract involvement in the motor dysfunction of adult-onset myotonic dystrophy type 1. *Sci Rep* 8, 15592. doi: 10.1038/s41598-018-34048-9
- Satterthwaite, T. D., Wolf, D. H., Loughhead, J., Ruparel, K., Elliott, M. A., Hakonarson, H., et al. (2012). Impact of in-scanner head motion on multiple measures of functional connectivity: relevance for studies of neurodevelopment in youth. *Neuroimage* 60, 623–632. doi: 10.1016/j.neuroimage.2011.12.063
- Schmahmann, J. D. (2019). The cerebellum and cognition. *Neurosci. Lett.* 688, 62–75. doi: 10.1016/j.neulet.2018.07.005
- Serra, L., Bianchi, G., Bruschini, M., Giulietti, G., Domenico, C. D., Bonarota, S., et al. (2020a). Abnormal cortical thickness is associated with deficits in social cognition in patients with myotonic dystrophy type 1. *Front. Neurol.* 11:113. doi: 10.3389/fneur.2020.00113
- Serra, L., Cercignani, M., Bruschini, M., Cipolletti, L., Mancini, M., Silvestri, G., et al. (2016a). “I know that you know that I know”: neural substrates associated with social cognition deficits in DM1 patients. *PLoS One* 11:e0156901. doi: 10.1371/journal.pone.0156901
- Serra, L., Mancini, M., Silvestri, G., Petrucci, A., Masciullo, M., Spanò, B., et al. (2016b). Brain connectomics' modification to clarify motor and nonmotor features of myotonic dystrophy type 1. *Neural Plast.* 2016:2696085. doi: 10.1155/2016/2696085
- Serra, L., Scocchia, M., Meola, G., D'Amelio, M., Bruschini, M., Silvestri, G., et al. (2020b). Ventral tegmental area dysfunction affects decision-making in patients with myotonic dystrophy type-1. *Cortex* 128, 192–202. doi: 10.1016/j.cortex.2020.03.022
- Serra, L., Silvestri, G., Petrucci, A., Basile, B., Masciullo, M., Makovac, E., et al. (2014). Abnormal functional brain connectivity and personality traits

- in myotonic dystrophy type 1. *JAMA Neurol.* 71, 603–611. doi: 10.1001/jamaneurol.2014.130
- Sugiyama, A., Sone, D., Sato, N., Kimura, Y., Ota, M., Maikusa, N., et al. (2017). Brain gray matter structural network in myotonic dystrophy type 1. *PLoS One* 12:e0187343. doi: 10.1371/journal.pone.0187343
- Theadom, A., Rodrigues, M., Roxburgh, R., Balalla, S., Higgins, C., Bhattacharjee, R., et al. (2014). Prevalence of muscular dystrophies: a systematic literature review. *Neuroepidemiology* 43, 259–268. doi: 10.1159/000369343
- Toth, A., Lovadi, E., Komoly, S., Schwarcz, A., Orsi, G., Perlaki, G., et al. (2015). Cortical involvement during myotonia in myotonic dystrophy: an fMRI study. *Acta Neurol. Scand.* 132, 65–72. doi: 10.1111/ane.12360
- van Dorst, M., Okkersen, K., Kessels, R. P. C., Meijer, F. J. A., Monckton, D. G., van Engelen, B. G. M., et al. (2019). Structural white matter networks in myotonic dystrophy type 1. *Neuroimage Clin.* 21:101615. doi: 10.1016/j.nicl.2018.101615
- Welniarz, Q., Gallea, C., Lamy, J. C., Méneret, A., Popa, T., Valabregue, R., et al. (2019). The supplementary motor area modulates interhemispheric interactions during movement preparation. *Hum. Brain Mapp.* 40, 2125–2142. doi: 10.1002/hbm.24512
- Xu, W., Chen, S., Xue, C., Hu, G., Ma, W., Qi, W., et al. (2020). Functional MRI-specific alterations in executive control network in mild cognitive impairment: an ALE meta-analysis. *Front. Aging. Neurosci.* 12:578863. doi: 10.3389/fnagi.2020.578863
- Xue, C., Qi, W., Yuan, Q., Hu, G., Ge, H., Rao, J., et al. (2021). Disrupted dynamic functional connectivity in distinguishing subjective cognitive decline and amnesic mild cognitive impairment based on the triple-network model. *Front. Aging Neurosci.* 13:711009. doi: 10.3389/fnagi.2021.711009
- Yan, C. G., Wang, X. D., Zuo, X. N., and Zang, Y. F. (2016). DPABI: data processing & analysis for (resting-state) brain imaging. *Neuroinformatics* 14, 339–351. doi: 10.1007/s12021-016-9299-4
- Yoo, W. K., Park, Y. G., Choi, Y. C., and Kim, S. M. (2017). Cortical thickness and white matter integrity are associated with CTG expansion size in myotonic dystrophy type I. *Yonsei Med J* 58, 807–815. doi: 10.3349/ymj.2017.58.4.807
- Zang, Y. F., He, Y., Zhu, C. Z., Cao, Q. J., Sui, M. Q., Liang, M., et al. (2007). Altered baseline brain activity in children with ADHD revealed by resting-state functional MRI. *Brain Dev.* 29, 83–91. doi: 10.1016/j.braindev.2006.07.002
- Zanigni, S., Evangelisti, S., Giannoccaro, M. P., Oppi, F., Poda, R., Giorgio, A., et al. (2016). Relationship of white and gray matter abnormalities to clinical and genetic features in myotonic dystrophy type 1. *Neuroimage Clin.* 11, 678–685. doi: 10.1016/j.nicl.2016.04.012
- Zeng, L. L., Wang, D., Fox, M. D., Sabuncu, M., Hu, D., Ge, M., et al. (2014). Neurobiological basis of head motion in brain imaging. *Proc. Natl. Acad. Sci. U.S.A.* 111, 6058–6062. doi: 10.1073/pnas.1317424111
- Zou, Q. H., Zhu, C. Z., Yang, Y., Zuo, X. N., Long, X. Y., Cao, Q. J., et al. (2008). An improved approach to detection of amplitude of low-frequency fluctuation (ALFF) for resting-state fMRI: fractional ALFF. *J. Neurosci. Methods* 172, 137–141. doi: 10.1016/j.jneumeth.2008.04.012
- Zuo, X. N., Di Martino, A., Kelly, C., Shehzad, Z. E., Gee, D. G., Klein, D. F., et al. (2010). The oscillating brain: complex and reliable. *Neuroimage* 49, 1432–1445. doi: 10.1016/j.neuroimage.2009.09.037

Conflict of Interest: The authors declare that the research was conducted in the absence of any commercial or financial relationships that could be construed as a potential conflict of interest.

The editor G-YY has declared a shared parent affiliation with the authors PH, X-HL, S-DC, JL, LC, and H-YZ at the time of review.

Publisher's Note: All claims expressed in this article are solely those of the authors and do not necessarily represent those of their affiliated organizations, or those of the publisher, the editors and the reviewers. Any product that may be evaluated in this article, or claim that may be made by its manufacturer, is not guaranteed or endorsed by the publisher.

Copyright © 2021 Huang, Luan, Xie, Li, Chen, Liu, Jia, Cao and Zhou. This is an open-access article distributed under the terms of the Creative Commons Attribution License (CC BY). The use, distribution or reproduction in other forums is permitted, provided the original author(s) and the copyright owner(s) are credited and that the original publication in this journal is cited, in accordance with accepted academic practice. No use, distribution or reproduction is permitted which does not comply with these terms.